# Two-gradient direction FXLMS: An Adaptive Active Noise Control Algorithm with Output Constraint

**DongYuan Shi**[1]

Digital Signal Processing Lab, School of Electrical and Electronic Engineering, Nanyang Technological University, SINGAPORE 639798

**Woon-Seng Gan**

Digital Signal Processing Lab, School of Electrical and Electronic Engineering, Nanyang Technological University, SINGAPORE 639798

**Bhan Lam**

Digital Signal Processing Lab, School of Electrical and Electronic Engineering, Nanyang Technological University, SINGAPORE 639798

**Chuang Shi**

School of Electronic Engineering, University of Electronic Science and Technology of China, Chengdu, Sichuan, CHINA 611731

[1] Electronic mail: DSHI003@e.ntu.edu.sg; Postal Address: Digital Signal Processing Lab, School of Electrical and Electronic Engineering, Nanyang Technological University, Singapore 639798, Singapore

**Abstract**

Active noise control (ANC) is broadly used to cancel the unwanted disturbance in different fields because of its excellent performance in abating low-frequency noise. In practice, however, the limited driving capability of actuators restrict the maximum output power of ANC systems. Once the driving signal of the ANC system exceeds these limitations, the inherent nonlinearity of the actuators will deteriorate the noise reduction and may result in the divergence of the adaptive algorithm. Hence, the two-gradient direction filtered-x least mean square (2GD-FXLMS) algorithm based on the optimal Kuhn-Tucker solution with the output constraint is proposed in this paper. This algorithm has the advantage of minimizing system overdriving, maintaining a specified power budget, and enhancing system stability. Compared to existing output-constrained adaptive algorithms, this proposed algorithm has the same computational complexity as the conventional FXLMS algorithm, while maintaining a stricter output constraint that minimizes the saturation distortion.

Index Terms- Saturation distortion, constrained optimization, Kuhn-Tucker solution, nonlinear active noise control, filtered-x least mean square algorithm, Hemstitching method.

## 1. Introduction

Conventional unconstrained adaptive algorithms are widely used in active noise control (ANC) systems [1–7]. The steady-state output of these algorithms usually drives actuators (for example, the combination of loudspeakers and amplifiers) to minimize the residual sound pressure level in a specified area. The actuators, however, have limited output capacity, reducing the effectiveness of conventional adaptive algorithms in handling large amplitude output signals [8]. In the case of output saturation, the mean square error (MSE) surface of the linear adaptive algorithms severely deforms as the degree of nonlinearity increases [9]. High degree of nonlinearity leads to the divergence of the adaptive algorithm [10], resulting in notable distortion [8]. Therefore, the saturation problem often limits the practical implementation of ANC solutions for suppressing loud noises [11].

In general, the nonlinear adaptive algorithm seems to be an effective solution to overcome the nonlinearity incurred in an ANC system [12]. When the actuators are partially overdriven, a typical nonlinear ANC algorithm either uses a truncated Volterra series [13,14] or a functional link artificial neural network (FLANN) [15,16] to improve the noise reduction performance and convergence speed [12,17]. Some other algorithms, such as the fuzzy adaptive algorithm, due to their self-tuning capability for the free parameters during the updating progress, also shows promise to handle the distortion of sensors and actuators [18,19]. However, the huge computational expense of the nonlinear ANC algorithms undermines their practicality. More importantly, when the power of the optimum control signal is greater than the output threshold of the actuator, neither the linear nor nonlinear ANC algorithms can provide sufficient power to cancel the disturbance [8,9]. If the anti-noise signal incompletely cancels the disturbance, the residual error accumulates in the weights of the control filter and may result in overflow [20]. Therefore, the nonlinear adaptive algorithm without any constraints may not be the desired solution for the saturation problem of ANC systems, in the case when actuators are severely overdriven.

A noteworthy strategy is to constrain the output amplitude of the control filter, which limits the maximum output level, prevents the actuators from being overdriven, and maintains a specified power budget [21–23]. For example, a clipping algorithm reported in [20] merely truncates the part of the output signal above the maximum output value at the expense of stability and convergence speed. Output constraint algorithms can be broadly classified into two categories: (1. cost function modification, which is exemplified by the leaky filtered-x least mean square

(Leaky FXLMS) algorithm [24], and (2. search direction modification methods [20]. The leaky FXLMS algorithm defines a new cost function by introducing a leakage or penalization factor that confines the control effort and stabilizes the adaptation [10,25]. However, its noise reduction occurs across all frequencies, resulting in a large, steady-state convergence error [26]. Improved leaky-type FXLMS algorithms introduce constraints into the frequency-domain implementation of the LMS algorithms, where only specific bins that violate constraints are penalized without severely affecting other frequencies [26–28]. The steady-state performances of these leaky-type FXLMS algorithms are easily affected by the empirical choice of the penalty coefficient [28]. Moreover, there is no guarantee that the output signal adheres to the imposed constraints [10].

Algorithms in [20,29,30] modify the search direction by using the gradient projection method [31,32], which concurrently rescales the output signal and control filter weights when the output violates the constraint. Those algorithms can ensure the control filter converges to an optimal solution under any specified power budget. Stability is achievable without pre-set penalty coefficient but at the cost of incurring more division and multiplying operations than the conventional FXLMS. Therefore, this paper proposes the two-gradient direction filtered-x least mean square (2GD-FXLMS) algorithm based on the Hemstitching method [33], which prevents the output saturation of the actuator while maintaining the same order of computational complexity as the conventional FXLMS algorithm [34].

The paper is organized as follows. Section 2 presents an overview of the existing ANC algorithms with output constraint. In addition, an improved objective function with the optimal solution is proposed, along with its minimum mean square error (MMSE) analysis. Section 3 proposes the 2GD-FXLMS algorithm to achieve the optimal solution based on the improved objective function, without increasing the computational complexity from the conventional FXLMS algorithm. Section 4 analyzes its computational complexity in detail. Lastly, simulation and testing results based on single-in/single-out (SISO) ANC are discussed in Section 5.

## 2. Output-constrained FXLMS

The block diagram of an adaptive feedforward ANC system is shown in Fig. 1. The signal $x(n)$ is the reference signal directly retrieved from the primary source in this paper, and the residual error signal $e(n)$ is the acoustic superposition in the air of the anti-noise $y'(n)$ and the disturbance $d(n)$. The control signal $y(n)$ is the output of the control filter $W(z)$. The transfer function $P(z)$ represents the combined physical path from the primary source to the error sensor. $S(z)$ is the transfer function of the secondary path from the output of the control filter $W(z)$ to the input of the error sensor, and it can be estimated by an adaptive filter $\hat{S}(z)$ using either off-line or online secondary path modeling methods [35].

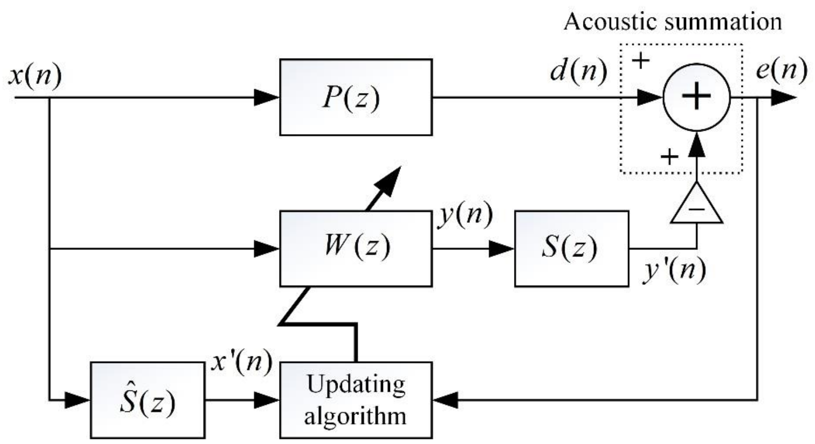


Fig. 1. Block diagram of the adaptive feedforward ANC system [4].

The adaptive ANC algorithm aims to minimize the power of the residual error $e(n)$. In practice, the adaptive algorithm must incorporate the output constraint so that the ANC system can manage a power budget, suppress the saturation of the actuator, and maintain the system stability. This is a constraint optimization problem. There are two common strategies to solve this constraint optimization problem: (1. through the cost function modification [36], and (2. changing the direction of the error gradient [29].

### 2.1 Cost function modification

The first strategy is to modify the cost function of the mean square error, as exemplified by the leaky FXLMS algorithm [24,37],

$$J(n) = e^2(n) + \gamma \mathbf{w}^T(n)\mathbf{w}(n)\,, \tag{1}$$

where $\gamma$ is the leakage factor (to mitigate the coefficient overflow problem, $\gamma \in (0,0.1)$; otherwise to constraint the output power, $\gamma > 0.1$) [38]. The vector of the control filter is expressed by $\boldsymbol{w}(n) = [w_0(n), w_1(n), \ldots, w_{M-1}(n)]^T$, where $T$ denotes the transpose function, and $M$ is the length of the control filter. The coefficient updating equation can be obtained by using the gradient descent method [39]

$$\mathbf{w}(n+1) = (1-\mu\gamma)\mathbf{w}(n) + \mu e(n)\mathbf{x}'(n)\,, \tag{2}$$

where $\mu$ is the step size of adaptation, and $\mathbf{x}'(n) = [x'(n), x'(n-1), \ldots, x'(n-M+1)]^T$ is the vector of the filtered reference signal, which is derived from the convolution of

$$x'(n) = \sum_{l=0}^{L-1} \hat{s}_l x(n-l)\,, \tag{3}$$

where $\hat{s}_l$ is the $l$th coefficient of the filter $S(z)$, whose length is $L$. In Eqs. (1) and (2), the leakage factor controls the "tightness" of the penalty for the cost function. If the selected leakage factor is significant, the control output may not be sufficiently large for satisfactory noise reduction. In contrast, if the selected leakage is trivial, the control output may violate the constraint and result in a saturation problem. Moreover, the optimal leakage factor depends on specific applications. Therefore, the leakage factor potentially causes instability to the ANC system and requires unnecessary complexity for practical implementation. Other algorithms based on penalty method even incurs higher computational complexity [23,25,27,28,40,41].

### 2.2 Search direction modification

An alternate strategy is the direction modification method, which does not alter the cost function. In this strategy, some algorithms search for the optimal solution along the constraints [20], while others search between the constraints and the feasible region [31], [33]. The typical example based on this strategy is the rescaling algorithm, which is given by

$$\begin{aligned}&\mathbf{w}(n+1)=\mathbf{w}(n)+\mu e(n)\mathbf{x}'(n),\\&y(n+1)=[x(n+1),x(n),\cdots,x(n-M+2)]^T\mathbf{w}(n+1).\end{aligned} \tag{4}$$

If $|y(n+1)|>C$, then

$$\begin{aligned}&\mathbf{w}(n+1)=\mathbf{w}(n+1)[C/|y(n+1)|],\\&y(n+1)=y(n+1)[C/|y(n+1)|],\end{aligned} \tag{5}$$

where $|\cdot|$ denotes the absolute value, and $C$ is the maximum output magnitude of the amplifier that can be obtained from its specification, circuit simulation or real measurement.

The rescaling algorithm adopts a gradient projection method to rescale the weights of the control filter and the output signal when the filter output violates the constraint. This step ensures that the adaptive algorithm eventually converges to the optimal solution (Kuhn-Tucker solution) under the constraint [42]. In contrast to the conventional FXLMS algorithm, the rescaling algorithm requires more multiplications and divisions, which increases with the length of the control filter and the control channels leading to a lower system sampling rate in the practical implementation of ANC.

### 2.3 Proposed objective function and its optimal solution

To obtain the optimal solution of the output-constrained adaptive algorithm, we reconstruct an optimization problem with inequality constraints given by

$$\begin{aligned} &\min J(\mathbf{w}) = E\left[\left|d(n) - \sum_{l=0}^{L-1} s_l \mathbf{w}^T(n-l)\mathbf{x}(n-l)\right|^2\right] \\ &s.t.\ g(\mathbf{w}) = E\left[\left|\mathbf{w}^T(n)\mathbf{x}(n)\right|^2\right] \le \rho^2, \end{aligned} \tag{6}$$

where $E[\cdot]$ and $|\cdot|^2$ denote the expectation operation and absolute value, respectively. $s_l$ is the $l$th coefficient of the filter $S(z)$ whose length is $L$, and $\mathbf{x}(n) = [x(n), x(n-1), \ldots, x(n-M+1)]^T$ is the reference signal vector. The cost function in Eq. (6) is the same as the conventional FXLMS algorithm, which aims to minimize the mean square error. In addition, the cost function must be subjected to an inequality constraint, whose average output power of ANC system must be less than the limit, $\rho^2$ for all $\rho > 0$.

The optimal solution $\mathbf{w}_o$ of Eq. (6) is derived in Appendix A as,

$$\mathbf{w}_o = (\lambda_o \mathbf{R}_{xx} + \mathbf{R}_{x'x'})^{-1}\mathbf{P}_{dx'}, \tag{7}$$

where $\mathbf{R}_{xx}$ and $\mathbf{R}_{x'x'}$ are autocorrelation matrix of the reference signal $x(n)$ and filtered reference signal $x'(n)$, respectively; $\mathbf{P}_{dx'}$ is the cross-correlation vector $E[d(n)\mathbf{x}'(n)]$. Note that $\lambda_o$ is the Lagrangian factor and

$$\lambda_o = \frac{E\{y_o'(n)[d(n) - y_o'(n)]\}}{\rho^2} \ge 0, \tag{8}$$

where the optimal anti-noise $y_0'(n) = \sum_{l=0}^{L-1} s_l \boldsymbol{w}^T(n-l)\boldsymbol{x}(n-l)$. Specifically, when $\lambda_0$ equals to 0, the optimal solution of the control filter reduces to

$$\mathbf{w}_o|_{\lambda_o=0} = \mathbf{R}_{x'x'}^{-1}\mathbf{P}_{dx'} \tag{9}$$

which is the optimal weight vector of the Wiener-Hopf equations [43]. The optimal solution indicates that the anti-noise signal completely cancels the disturbance $d(n)$ within the output constraint. Therefore, the solution of the constrained optimization in Eq. (6) would reduce to the Wiener-Hopf solution, if the output power remains in the constraint.

### 2.4 Minimal mean square error (MMSE) analysis

The MSE function of an ANC system can be stated as

$$J(\mathbf{w}) = E\left[d(n)^2\right] - \mathbf{P}_{dx'}^T\mathbf{w} - \mathbf{w}^T\mathbf{P}_{dx'} + \mathbf{w}^T\mathbf{R}_{x'x'}\mathbf{w} \tag{10}$$

If $\lambda_o > 0$, the minimum mean square error (MMSE) is derived in Appendix B as

$$J_{\min} = E\left[d(n)^2\right] - \left(2\lambda_o + \sum_{l=0}^{L-1} s_l^2\right)\rho^2 \tag{11}$$

In Eq. (11), when $\lambda_o > 0$, a bigger threshold $\rho^2$ can lead to a smaller MSE. If $\lambda_o = 0$, substituting Eq. (9) into Eq. (10) yields

$$J_{\min}(\mathbf{w}_o) = E\left[d(n)^2\right] - \mathbf{P}_{dx'}^T\mathbf{w}_o, \tag{12}$$

which is as the same as the MSE of the conventional FXLMS algorithm [44].

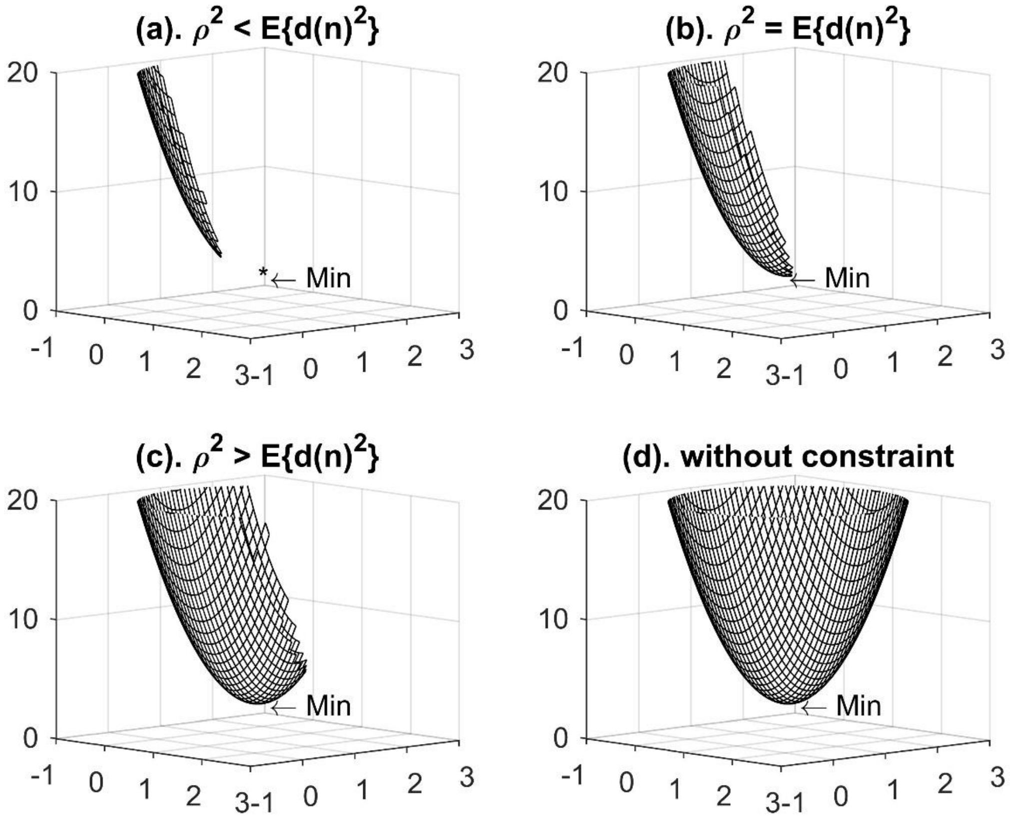


Fig. 2. Mean square error surface of the adaptive algorithm with output constraint when the threshold is (a) less than the power of the disturbance, (b) equals to the power of the disturbance, and (c) larger than the power of the disturbance. The case without constraint is shown in (d).

From Eqs. (11) and (12), it is obvious that the threshold $\rho^2$ relates to the MSE, which is shown in Fig. 2. If $\rho^2$ is smaller than the power of the noise disturbance $d(n)$, $E[d(n)^2]$, the MSE cannot achieve the minimum solution of the algorithm without constraint as depicted in Fig. 2(a). The MSE performance is improved as $\rho^2$ increases. When $\rho^2$ equals to $E[d(n)^2]$, the MMSE is as the same as the algorithm without constraint and locates the minimum point on the bound of the MSE surface, as shown in Fig. 2(b). If $\rho^2$ surpasses the power of the disturbance noise, the adaptive algorithm with constraint can gain the same noise reduction as the conventional FXLMS algorithm, as shown in Fig. 2(c). However, this threshold is decided by the driving capability of the secondary source, which is measured by experiments. Fig. 2(d) illustrates the optimal solution of FXLMS algorithm without constraint.

## 3. Output-constrained two-gradient direction FXLMS (2GD-FXLMS) algorithm

Although the optimal solution of the output-constrained control filter has been derived in Eq. (7), the real-time implementation incurs high computation load due to matrix inversion. Hence, we proposed a time-iterative algorithm based on the hemstitching method [33]. The algorithm searches for the optimal solution along the negative gradient direction of the cost function or the output constraint, depending on the condition, which is described in this section.

When the average output power of the control filter is within the constraint ($E[y(n)^2] = E[|\boldsymbol{w}^T(n)\boldsymbol{x}(n)|^2] \leq \rho^2$), the weight update is given by

$$\mathbf{w}(n+1) = \mathbf{w}(n) - \frac{1}{2}\mu\frac{\nabla J(\mathbf{w})}{\|\nabla J(\mathbf{w})\|}. \tag{13}$$

In contrast, when the average output power exceeds the constraint ( $g(\boldsymbol{w}) = E[|\boldsymbol{w}^T(n)\boldsymbol{x}(n)|^2] > \rho^2$), the weight update changes to

$$\mathbf{w}(n+1) = \mathbf{w}(n) - \frac{1}{2}\mu\frac{\nabla g(\mathbf{w})}{\|\nabla g(\mathbf{w})\|}, \tag{14}$$

where $\nabla$ and $\|\cdot\|$ denote the differentiation operator and the Euclidean distance, respectively. Since the statistics of the autocorrelation matrix of the reference and the filtered reference signal cannot be directly obtained in practical applications, we approximate the gradient of the cost function and the constraint by their instantaneous value, as

$$\nabla J(\mathbf{w}) \approx \frac{\partial[d(n)-\sum_{l=0}^{L} s_l \mathbf{w}^T(n-l)\mathbf{x}(n-l)]^2}{\partial \mathbf{w}(n)} \\ \approx -2e(n)\sum_{l=0}^{L} s_l \mathbf{x}(n-l) \\ \approx -2e(n)\mathbf{x}'(n), \tag{15}$$

and

$$\nabla g(\mathbf{w}) \approx \frac{\partial[\mathbf{w}^T(n)\mathbf{x}(n)\mathbf{x}^T(n)\mathbf{w}(n)]}{\partial \mathbf{w}(n)} \\ \approx 2y(n)\mathbf{x}(n). \tag{16}$$

respectively. By substituting Eqs. (15) and (16) into Eqs. (13) and (14), respectively, and by replacing the normalized gradient and average power constraint with the instantaneous gradient and amplitude constraint, the update equation can now be expressed as

$$\mathbf{w}(n+1) = \mathbf{w}(n) + \mu e(n)\mathbf{x}'(n), \tag{17}$$

when the output signal $|\mathrm{y(n)}| = |\mathbf{w}^{\mathrm{T}}(\mathrm{n})\mathbf{x}(\mathrm{n})| \leq \mathrm{C}$, while

$$\mathbf{w}(n+1) = \mathbf{w}(n) - \mu y(n)\mathbf{x}(n), \tag{18}$$

when the output signal $|\mathrm{y(n)}| = |\mathbf{w}^{\mathrm{T}}(\mathrm{n})\mathbf{x}(\mathrm{n})| > \mathrm{C}$. $C$ is the equivalent constraint of the output amplitude and can be measured by experiments or obtained from the technical specifications of the actuator and amplifier. If the output signal is a sine tone, $C$ equals to $\frac{\rho}{\sqrt{2}}$. It is noteworthy that, because we replaced the normalized step size $\frac{\mu}{2\|g(w)\|}$ with a constant step size $\mu$ in Eq. (18), the convergence speed and stability of the algorithm will be sensitive to the value of $\mu$ [45], which depends on the correlation statistics of the input data [46] and the constraint. If the $\mu$ is too small, then Eq. (18) cannot promptly adjust the control filter back to the feasible area after it violates the constraint, which will lead the distortion in the output signal; However, if $\mu$ is large, it will cause a bigger steady-state error in the algorithm. One potential solution is to use two different step sizes in Eqs. (17) and (18), but this requires an in-depth theoretical analysis and practical verifications, and is thus out of the research scope in this paper. Henceforth, the same step size will be used for both Eqs. (17) and (18).

As indicated in Eqs. (17) and (18), the weight of the control filter varies along the same direction as the FXLMS algorithm if the output signal is within its constraint. Once the output signal violates the constraint, it switches the gradient direction of the constraint so that the weight rebounds from the boundary, which reduces the output power. The weight update continues in this manner until it reaches the optimal solution. As the proposed algorithm updates along two gradient directions, it is named the two-gradient direction FXLMS (2GD-FXLMS). Since the constraint in Eq. (6) restricts the average output power, there is no guarantee that the instantaneous output power falls within the constraint, which results in saturation distortion. To solve this problem, the output signal is clipped when its amplitude is above the constraint. Hence, if $|y(n)| \leq C$ the output signal is given by

$$y_{out}(n) = y(n). \tag{19}$$

If $|y(n)| > C$, the output signal will become

$$y_{out}(n) = \begin{cases} C, & y(n) > 0 \\ -C, & y(n) < 0 \end{cases}, \tag{20}$$

where $y_{out}(n)$ is the clipped output signal.

## 4. An analysis on the computational complexity of the algorithm

Computational burden is a critical issue that should be taken into account when referring to the practical implementation of an adaptive algorithm. For a real-time platform, such as the digital signal processor (DSP) [47], the microcontroller unit (MCU) [48,49], the field programmable gate array (FPGA) [50] and so on, the burden is mainly brought on by multiplication/division, addition/subtraction in the execution of the algorithm. Compared to the conventional FXLMS algorithm, the 2GD-FXLMS algorithm has the same computational complexity (regarding the multiplication and addition), as illustrated in

Table 1.

Table 1. Comparison on the computational complexity of different algorithms

| Algorithm | Multiplication | Addition | Division |
|---|---|---|---|
| FXLMS | 2M+L+1 | 2M+L-2 | 0 |
| Leaky FXLMS | 3M+L+1 | 2M+L-2 | 0 |
| Rescaling Algorithm | 3M+L+2 | 2M+L-2 | 1 |
| 2GD-FXLMS | 2M+L+1 | 2M+L-2 | 0 |

However, the 2GD-FXLMS also requires several additional switches and one threshold, as shown in Fig. 3. When the output signal $y(n)$ exceeds the constraint, it will be clipped by the threshold. Meanwhile, the threshold triggers the switches to select the "Y" branch so that the weight update direction changes to reduce the output power until the output signal returns within the constraint. In contrast, if the output signal is within the constraint, the switches choose the "N" branch, which makes the algorithm search the optimal solution on the negative gradient direction of FXLMS algorithm.

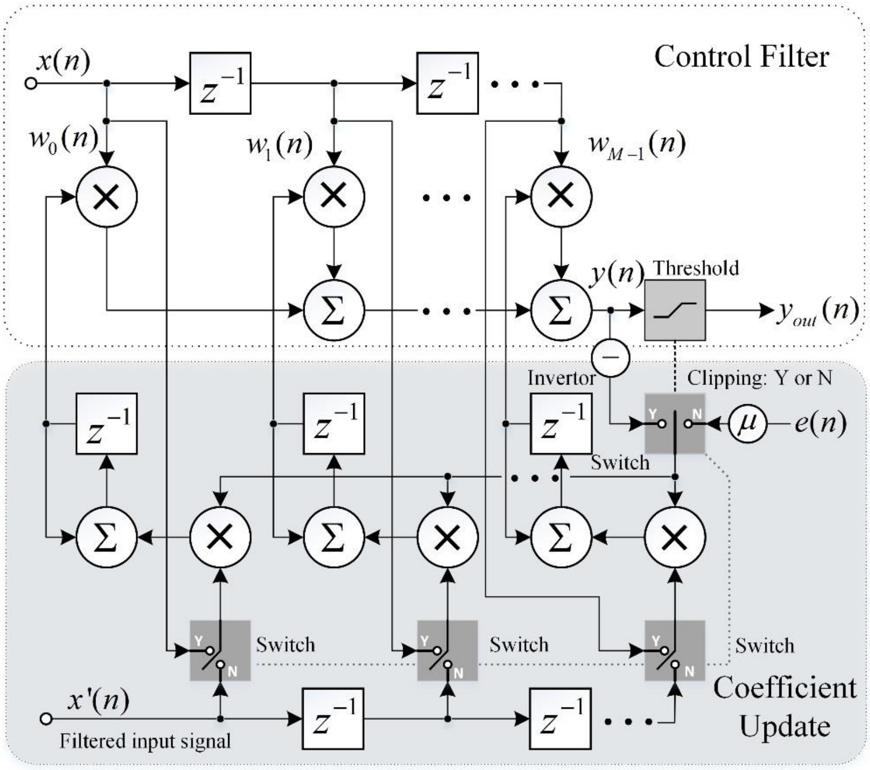


Fig. 3. The detailed block diagram of the 2GD-FXLMS algorithm.

To swap the two gradient directions of the 2GD-FXLMS algorithm in the processor, we can use some conditional statements, such as "if…else", as the pseudocode shows in Table 2. The conditional branch sentences usually costs few machine cycles, which can be ignored compared to the machine cycles used by addition, multiplication, and division operations [51]. When we implement the 2GD-FXLMS on the digital circuit, such as VLSI and FPGA, the mechanism of the switch in Fig. 3 can be realized by the multiplexer. The multiplexer is a basic component in the digital circuit and composes of few gates. Compared to the adder, multiplier, and divider, the number of gates used in the multiplexer can also be ignored [52]. Therefore, the additional complexity for the control part of the 2GD-FXLMS algorithm is trivial compared to the computational complexity of the conventional adaptive algorithm.

Table 2. Pseudocode of the proposed algorithm

| Two gradients FXLMS (2GD-FXLMS) algorithm |
| --- |
| Input : Reference signal $x(n)$ and error signal $e(n)$ |
| Output : Clipped output signal $y_{out}$ |

**Step 1** : $y(n) = \mathbf{w}^T(n)\mathbf{x}(n)$

$x'(n) = \hat{\mathbf{s}}^T \mathbf{x}(n)$

**Step 2** : If $|y(n)| \le C$

$\mathbf{w}(n+1) = \mathbf{w}(n) + \mu e(n)\mathbf{x}'(n)$

else

$\mathbf{w}(n+1) = \mathbf{w}(n) - \mu y(n)\mathbf{x}(n)$

**Step 3** : If $y(n) > C$

$y_{out} = C$

else if $y(n) < -C$

$y_{out} = -C$

else

$y_{out} = y(n)$

## 5. Simulation performance of the 2GD-FXLM algorithm

### 5.1 Control of simulated tonal noise

In the first simulation, we carried out a comparative study on the performance of FXLMS algorithm, leaky FXLMS algorithm, rescaling algorithm, and the proposed 2GD-FXLMS algorithm in a time-invariant system, through Figs. 4 to 7. The sampling frequency $f_s$ is set to 10 kHz, and the reference signal $x(n)$ is $2.15\sin(0.16\pi n)$. The primary and secondary path is chosen as $\mathbf{p} = [0.3,0.3]^T$ and $\mathbf{s} = [1,0]^T$, respectively. The step size $\mu$ of the adaptive algorithm is 0.05, and the output constraint $C$ is 0.75.

As illustrated in Fig. 4, the FXLMS algorithm (or the leaky FXLMS algorithm with leakage factor $\gamma = 0$) failed to control the amplitude of the output signal, while the leaky FXLMS algorithm with $\gamma = 0.25$, rescaling algorithm, and 2GD-FXLMS algorithm successfully confined the output signal within the output constraint.

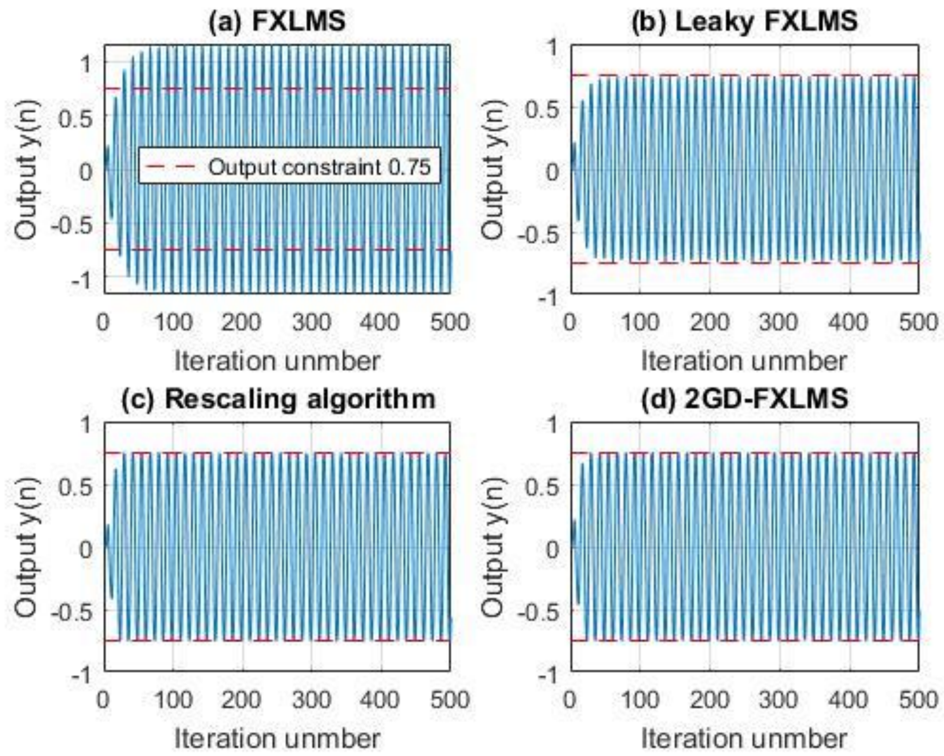


Fig. 4. The output signal of (a) FXLMS algorithm, (b) leaky FXLMS algorithm, (c) rescaling algorithm, and (d) 2GD-FXLMS algorithm.

In Fig. 5, the dashed red curve denotes the average power

$$E\left[\left|\mathbf{w}^{T}(n)\mathbf{x}(n)\right|^{2}\right]=\frac{C^{2}}{2}=0.28125, \tag{21}$$

which divides the solution surface into two parts: (1. The feasible region, where the average output power of the control filter is less than the value $\frac{C^2}{2}$, and contains the origin (0,0); and (2. the infeasible region, where the average output power of the control filter exceeds the value $\frac{C^2}{\sqrt{2}}$. Although the FXLMS algorithm converges to the optimal solution, as illustrated in Fig. 5(a), it is out of the feasible region, and hence, results in the average output power exceeding the power limitation. In contrast, the final solutions of the other algorithms are close to this average power constraint curve. Furthermore, the optimal solution with output constraint was derived from Eqs. (7) and (8) as

$$\mathbf{w}_o = \begin{pmatrix} 0.172 \\ 0.206 \end{pmatrix}. \tag{22}$$

In Fig. 5, the final solutions of these algorithms are $\boldsymbol{w}_{FXLMS} = [0.3,0.3]^{\mathrm{T}}$, $\boldsymbol{w}_{leaky} = [0.162,0.214]^{T}$, $\boldsymbol{w}_{rescaling} = [0.183,0.243]^{T}$, and $\boldsymbol{w}_{2GDFXLMS} = [0.169,0.204]^{T}$. Therefore, the 2GD-FXLMS is the closest to the Kuhn-Tucker's solution.

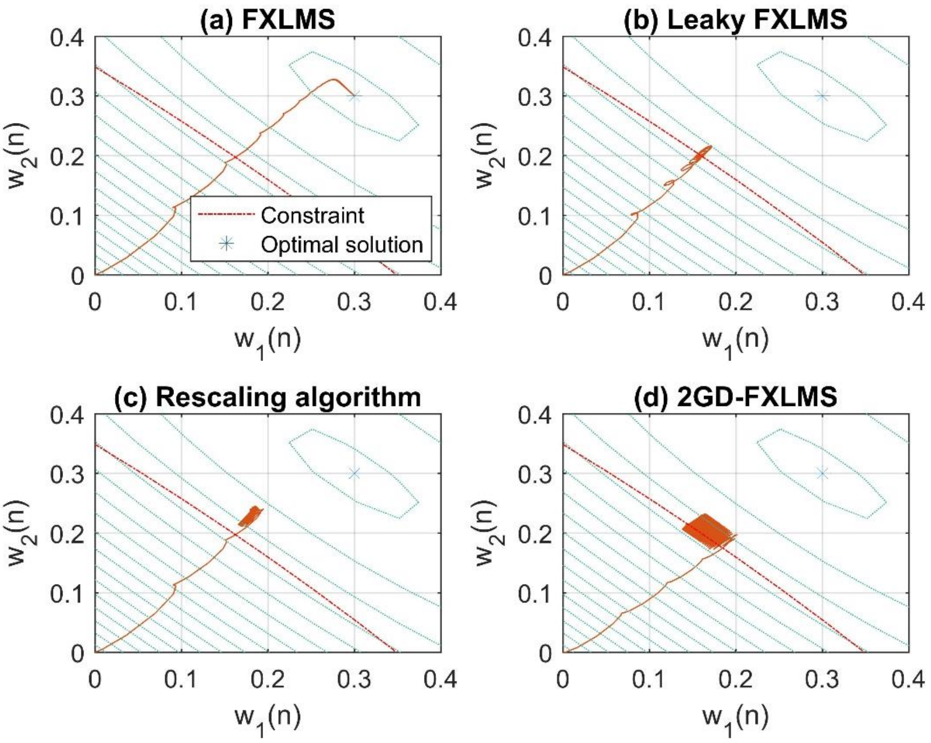


Fig. 5. The weight convergence path of the (a) FXLMS algorithm, (b) leaky FXLMS, (c) rescaling algorithm, and (d) 2GD-FXLMS algorithm against contours of the mean square error $E[e^2(n)]$, with the red curve denoting the constraint $E[|\mathbf{w}^T(n)\mathbf{x}(n)|^2] = 0.28125$ .

Since the leaky FXLMS, rescaling, and 2GD-FXLMS algorithms restricted the output signal in the presence of the constraint, it can be observed that the FXLMS algorithm has the smallest residual error, as shown in Fig. 6 The noise reduction after convergence was 8.1 dB, 8.9 dB, and 8.5 dB for leaky FXLMS, rescaling, and 2GD-FXLMS algorithms, respectively. The rescaling algorithm has the better noise reduction at the expense of slightly exceeding the average power limitation, as shown in Fig. 5(c). As one would expect, the FXLMS algorithm almost entirely canceled the noise at the expense of letting the output signal exceeding the constraint by a large margin, as illustrated in Fig. 4(a).

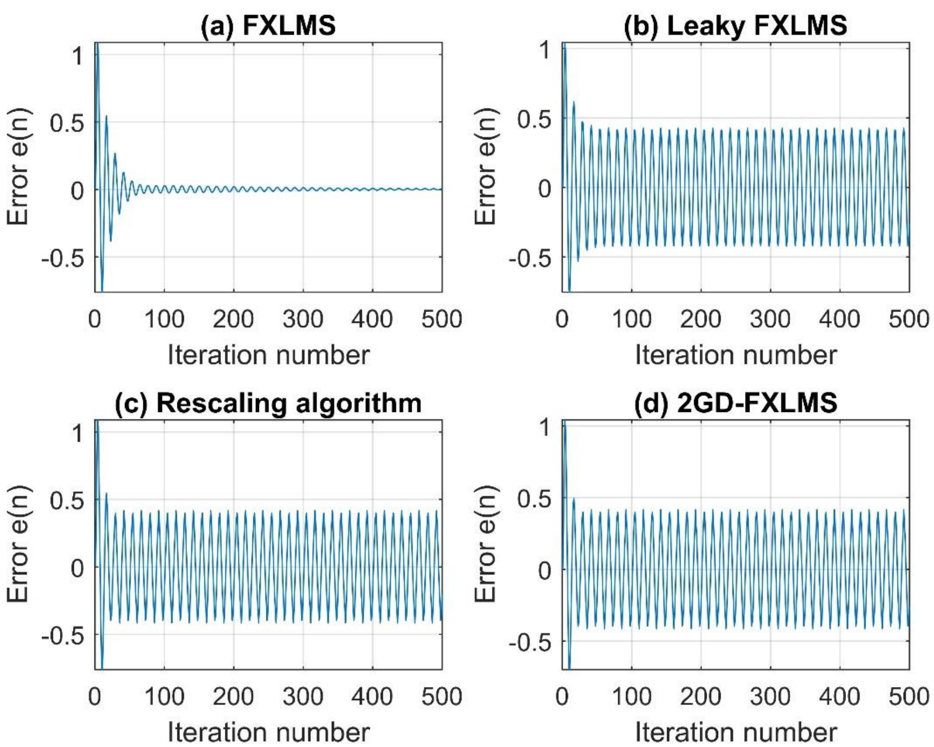


Fig. 6. The residual error of the FXLMS algorithm, leaky FXLMS algorithm, rescaling algorithm, and 2GD-FXLMS algorithm.

### 5.2 Control of simulated random noise

The performance of the three algorithms under a time-varying system using random noise as the reference signal is shown through Figs. 7 to 9. The mean value of the random noise used in the simulations is 0, and its standard deviation is 0.9. In the simulation, the primary path is a time-varying system with $\mathbf{p} = [0.25{,}0.35]^T$ for the first 1.5 seconds and then changes to $\mathbf{p} = [0.5{,}0]^T$ in the next 1.5 s, and $\mathbf{p} = [0{,}0.5]^T$ for the last 1.5 s, totalling 4.5 s. The secondary path remains unchanged with $\boldsymbol{s} = [1{,}0]^T$. The step size of the three algorithms is set to $\mu = 0.001$, and the leakage factor $\gamma$ in the leaky FXLMS algorithm is set to 0.5.

In Fig.7 (a), it is noted that the leakage factor $\gamma = 0.5$ can limit the amplitude of the output signal with the constraint of $C = 0.75$ for the first primary path but fails for the second and third primary paths. Therefore, the leaky FXLMS with a fixed leakage factor cannot fully guarantee that the output signal can always satisfy the output constraint for a time-varying system or for different primary paths. In contrast, the rescaling and 2GD-FXLMS algorithm successfully restricted the output signal within the constraint during the whole adaptation process, as shown in Fig. 7(b) and (c). These three algorithms successfully track the variation of the primary path, as illustrated in Fig. 8. Fig. 8 (d) depicts the distribution ratio of two gradient directions (GD1 and GD2) used in the 2GD-FXLMS algorithm during the adaptive control process. Moreover, 2GD-FXLMS has a smaller residual error than both the rescaling and leaky FXLMS algorithms, as shown in Fig. 9. Its average output power constraint performs better with broadband noise.

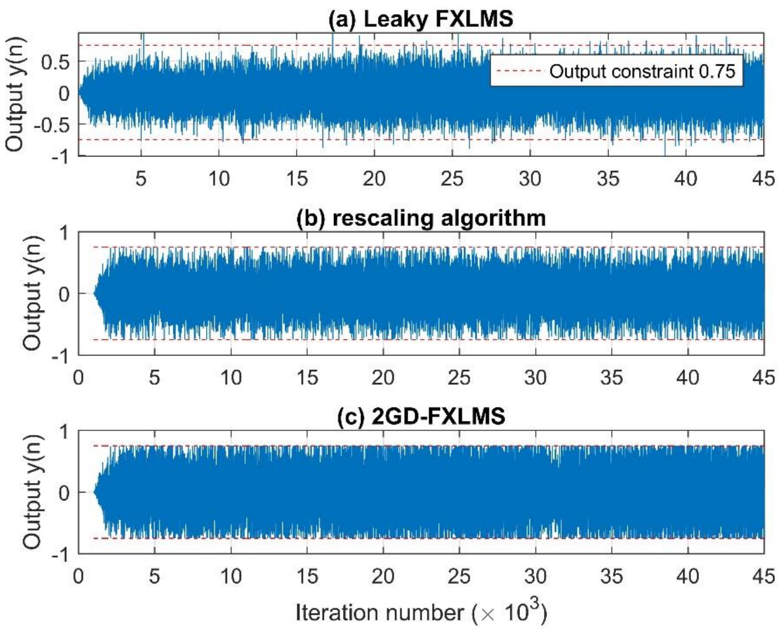


Fig. 7. The control filter output variation of the (a) leaky FXLMS, (b) rescaling, and (c) 2GD-FXLMS algorithms with a constraint of 0.75, as indicated by the dashed line.

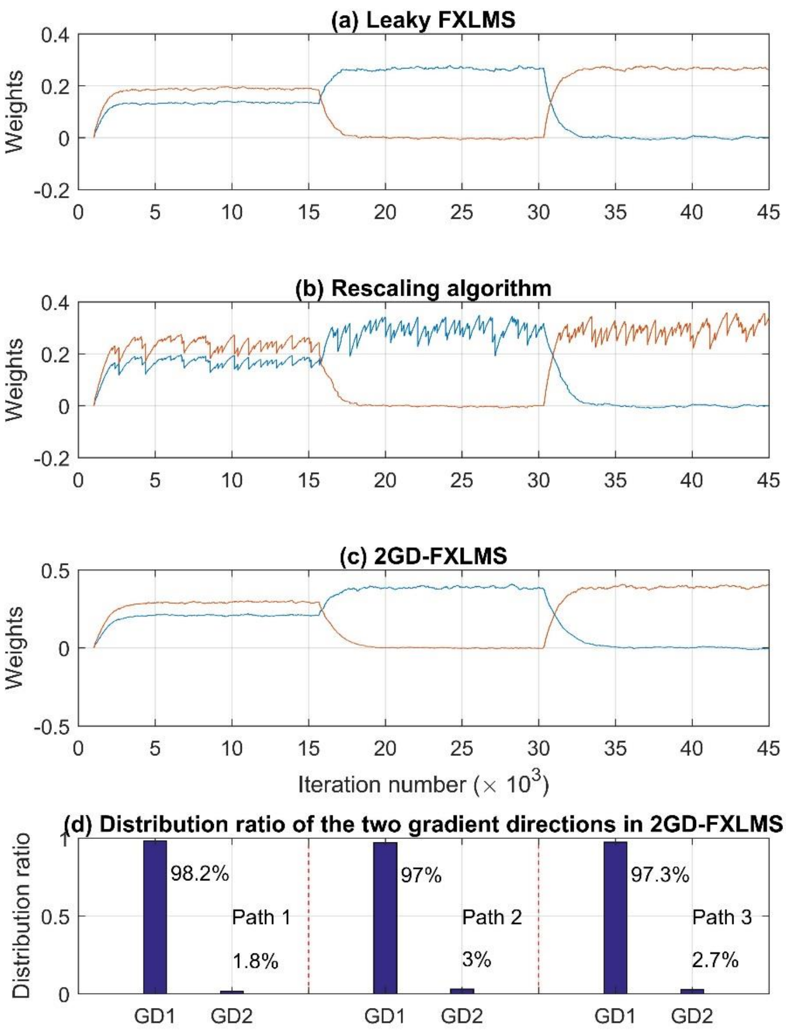


Fig. 8. The control filter weight variation of the (a) leaky FXLMS, (b) rescaling, and (c) 2GD-FXLMS algorithm, as a function of the number of iterations; and (d) the distribution ratio of the two gradient directions in 2GD-FXLMS.

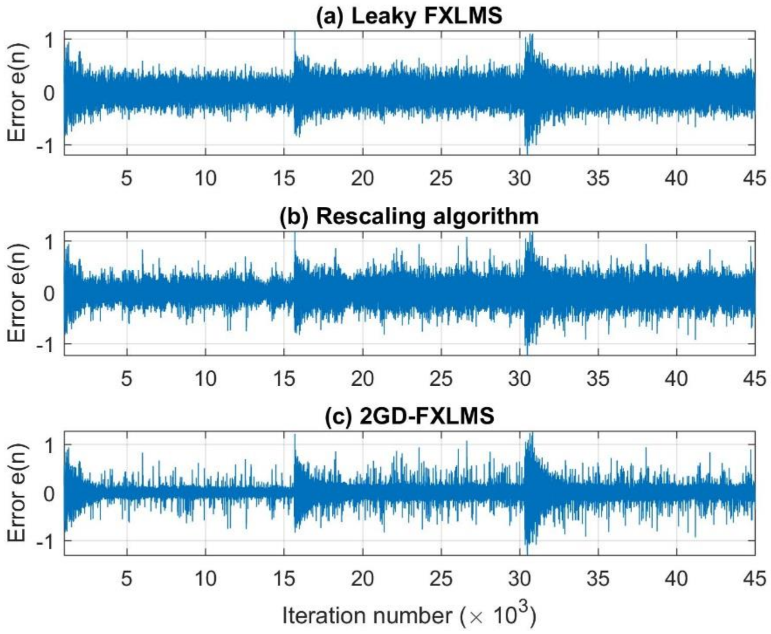


Fig. 9. The error signal variation of the (a) leaky FXLMS, (b) rescaling, and (c) 2GD-FXLMS algorithms, as a function of the number of iterations.

## 5.3 Tonal control in a single channel practical active control system

In the final simulation, we considered an actual single channel feedforward ANC system. The impulse responses of the primary path and secondary path are illustrated in Fig. 10 (a) and (b), respectively. In this system, the TDA2003 audio amplifier was used, whose output amplitude limit was 0.75 and gain was close to unity. Its input-output transfer function is approximated by an error function [9]

$$y(n)=\frac{5}{\sqrt{2\pi}}\int_{0}^{x(n)} e^{-\frac{\tau^2}{0.18}}d\tau\ , \qquad (23)^2$$

---

[2] For other error functions with different nonlinearities, the 2GD-FxLMS can still work well with a suitable constraint.

which is depicted in Fig. 10 (c). Due to $\lim_{x\to\pm\infty} y(n) = \pm 0.75$, this error function will truncate the signal whose amplitude is above 0.75. The sampling frequency $f_s$ is 10 kHz, and the reference signal $x(n)$ is $0.32\sin(0.1\pi n)$.

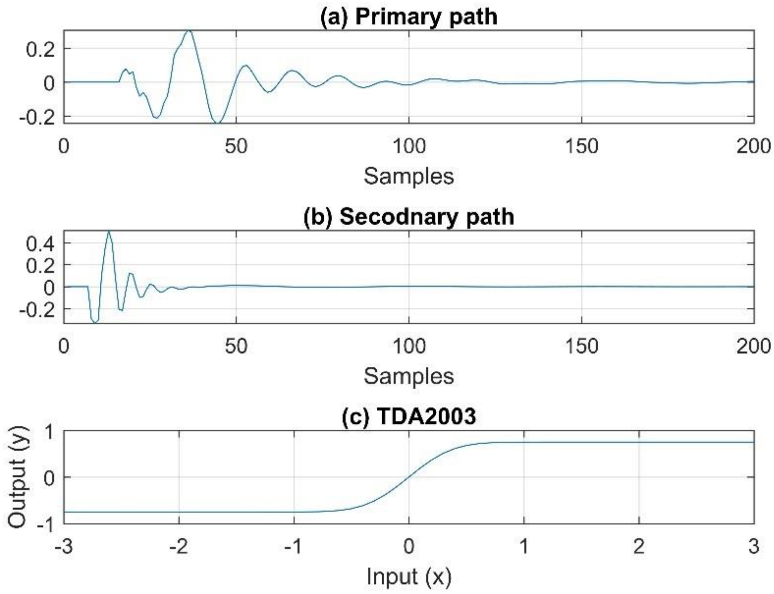


Fig. 10. The impulse response of the (a) primary path, and (b) secondary path, of a real ANC system, and (c) output value vs. the input value of the amplifier TDA2003.

In the simulation, the FXLMS, rescaling, and the 2GD-FXLMS algorithms have been deployed to cancel the noise disturbance. As the FXLMS algorithm did not restrict the output signal, the amplitude of the output signal quickly exceeded the constraint, as shown in Fig. 11 (a). The large output signal overdrives the amplifier, which causes the amplifier to distort the output signal and hence, generates significant distortions and harmonics in the residual error, as shown in Fig. 12 (b). In this case, the noise disturbance far exceeds the maximum signal of the secondary source, which results in a high residual error that pushed the filter weights increasingly beyond the limit. The harmonics of the residual error also increased and finally exceeded the power of the disturbance noise, pushing the total harmonic distortion (THD) to $-17.4$ dB (13.5 %). Even though the FXLMS algorithm reduced the noise disturbance by

23 dB, this came at the expense of increased harmonic distortions (e.g., 3rd harmonic distortion increased to 83 dB). Note that the power of the disturbance is just 83 dB as shown in Fig. 12 (a).

The leaky algorithm even with a large leaky factor $\gamma = 2$ failed to restrict the output signal within the constraint. Although the leaky FXLMS algorithm achieved an attenuation of 12 dB, as shown in Fig. 12 (c), its final output signal is slightly above the constraint, which resulted in obvious distortion in the residual error with a THD of $-18.6$ dB (11.7%).

The rescaling algorithm successfully confines the output signal within the output constraints, as illustrated in Fig. 11 (c). Its spectrum of the residual error after convergence is shown in Fig. 12(d). Despite the noise disturbance decreasing by 12 dB, some harmonics still exists in the residual error with a THD of $-34.4$ dB (1.9%).

Similar to the rescaling algorithm, the 2GD-FXLMS effectively restricts the output signal, as shown in Fig. 11 (d). Although its noise reduction is just 12 dB, only a minor third harmonic is observed in the residual error signal, as shown in Fig. 12 (e), and further exemplified by the low THD of $-55$ dB (0.2%). Its distribution ratio of two gradient directions shown in Fig. 12 (f) indicates that the algorithm spends 9.8 % of the time on restricting the output signal by using the second gradient direction. Therefore, this simulation highlights the capabilities of the 2GD-FXLMS algorithm in constraining the output signal, as well as in prohibiting the nonlinearity due to saturation in the ANC system.

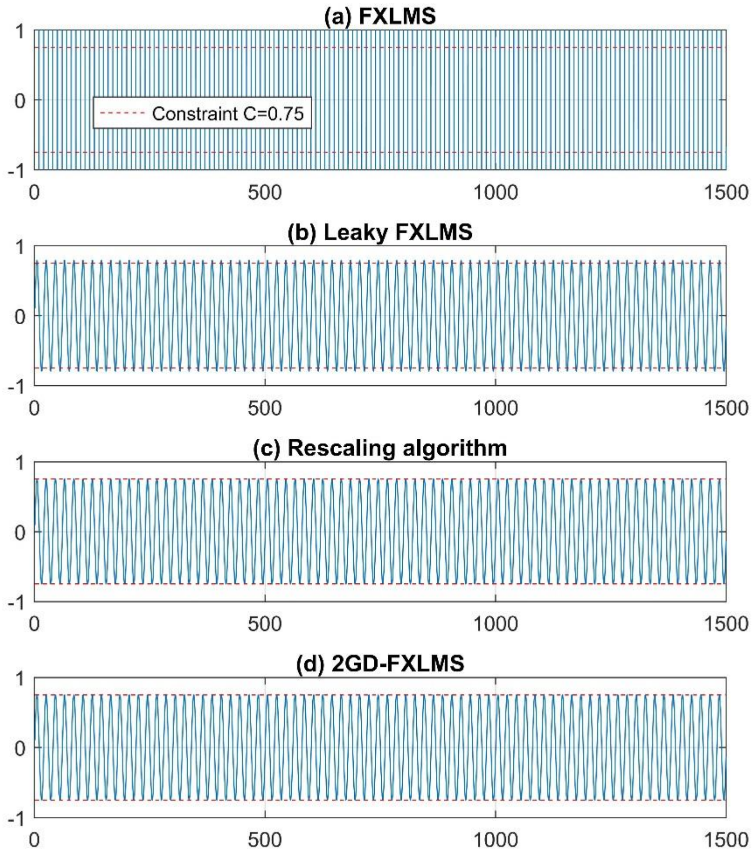


Fig. 11. The output signal of the (a) FXLMS algorithm, (b) leaky FXLMS algorithm, (c) rescaling algorithm, and (d) the 2GD-FXLMS algorithm, all as a function of the number of iterations.

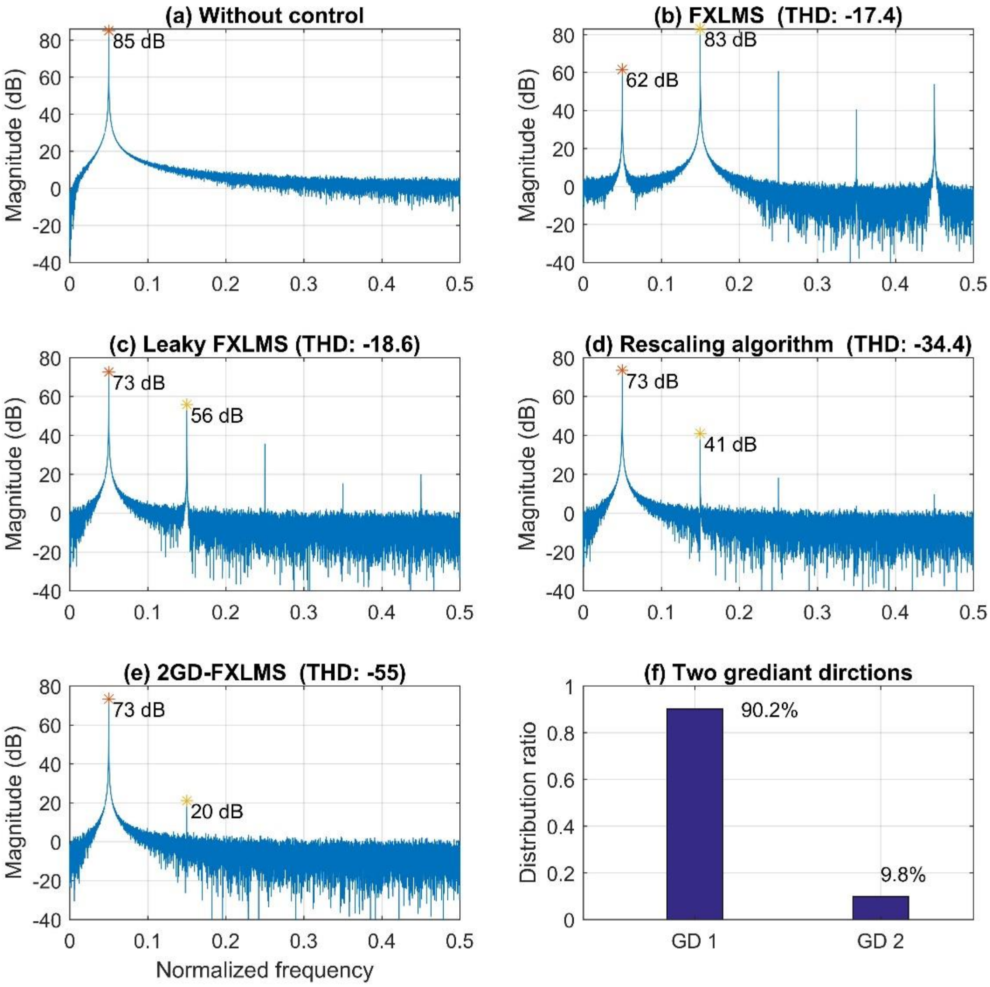


Fig. 12. The spectrum of the error signal for a real ANC system, (a) without control, (b) with FXLMS algorithm, (c) with leaky FXLMS algorithm, (d) with the rescaling algorithm, and (e) with the 2GD-FXLMS algorithm, all as a function of normalized frequency. The distribution ratio of two gradient directions in 2GD-FXLMS algorithm is shown in (f).

## 6. Discussion and Conclusion

This paper proposes a new adaptive algorithm with output constraint for practical active noise control systems. The new algorithm, the two-gradient direction FXLMS (2GD-FXLMS) algorithm, uses two gradient directions to update the weights of the control filter. When the output signal violates the constraint, the adaptive algorithm switches the weight update direction to reduce the power of the output signal.

Compared to other output constraint algorithms, the 2GD-FXLMS algorithm has the same order of computational complexity as the conventional FXLMS algorithm. In addition, it has a stricter output constraint, which can restrict the instantaneous amplitude and average power of the output signal at the same time. Therefore, it can be applied to mobile devices and portable equipment, where the output power of actuator and computation power of the processor is limited.

The proposed approach 1) prevents the actuator from being overdriven; 2) prohibits nonlinearity due to saturation; 3) improves the system stability and sound quality after the noise reduction. Simulations conducted with measured transfer responses of a real setup demonstrated its effectiveness in confining the system output under a specific power constraint, over other output constraint algorithms.

However, the overall performance of the 2GD-FXLMS algorithm is also influenced by its two steps. Hence, it would be more interesting and meaningful to carry out the further study on the steps of the 2GD-FXLMS in detail. Furthermore, the advantage of the 2GD-FXLMS algorithm in computational complexity also shows its promising usage in the multichannel ANC applications.

## 7.1 Appendix A: Proof of optimal solution existence

To solve the objective Eq. (6), we first construct a slack variable $\theta^2$,

$$\theta^2 = \rho^2 - g(\mathbf{w}). \tag{A1}$$

Next, we define a Lagrangian function based on Eq. (6) and slack variable as defined in Eq. (A1) as

$$L(\mathbf{w},\lambda,\theta) = J(\mathbf{w}) + \lambda[g(\mathbf{w}) + \theta^2 - \rho^2], \tag{A2}$$

where $\lambda$ ($\lambda \in \mathbb{R}$) is the Lagrangian factor. By using the Lagrangian necessary conditions [53], Eq. (A2) is differentiated with respect to $\mathbf{w}(n)$, $\lambda$ and $\theta$, respectively, and equated to 0.

$$\frac{\partial L(\mathbf{w},\lambda,\theta)}{\partial \mathbf{w}} = \frac{\partial J(\mathbf{w})}{\partial \mathbf{w}} + \lambda \frac{\partial g(\mathbf{w})}{\partial \mathbf{w}} = 0; \tag{A3}$$

$$\frac{\partial L(\mathbf{w},\lambda,\theta)}{\partial \lambda} = g(\mathbf{w}) + \theta^2 - \rho^2 = 0; \tag{A4}$$

$$\frac{\partial L(\mathbf{w},\lambda,\theta)}{\partial \theta} = 2\lambda\theta = 0. \tag{A5}$$

Next, the gradient of the cost function is given by

$$\begin{aligned}\frac{\partial J(\mathbf{w})}{\partial \mathbf{w}} &= \frac{\partial}{\partial \mathbf{w}(n)} E\left[ |\, d(n) - \mathbf{w}^T(n)\mathbf{X}(n)\mathbf{s}(n) |^2 \right] \\ &= \frac{\partial}{\partial \mathbf{w}(n)} E[d^2(n) - 2d(n)\mathbf{w}_o^T\mathbf{X}(n)\mathbf{s}(n) \\ &\quad + \mathbf{w}_o^T\mathbf{X}(n)\mathbf{s}(n)\mathbf{s}^T(n)\mathbf{X}^T(n)\mathbf{w}(n)] \\ &= -2\mathbf{P}_{dx'} + 2\mathbf{R}_{x'x'}\mathbf{w}(n),\end{aligned} \tag{A6}$$

where the vector $\mathbf{P}_{dx'}$ is $E[d(n)\mathbf{X}(n)\mathbf{s}]$, and the vector $\mathbf{R}_{x'x'}$ is $E[\mathbf{X}(n)\mathbf{s}\mathbf{s}^T\mathbf{X}^T(n)]$. The input signal matrix, of order $M \times L$, is stated as $\mathbf{X}(n) = [\mathbf{x}(n), \mathbf{x}(n-1), \ldots, \mathbf{x}(n-L+1)]$. The coefficient vector is $\boldsymbol{s} = [s_0, s_1, \ldots, s_{L-1}]^T$, where $s_l$ is the $l$th coefficient of the secondary path $S(z)$. The gradient of the output constraint can be written as

$$\begin{aligned}\frac{\partial g(\mathbf{w})}{\partial \mathbf{w}} &= \frac{\partial}{\partial \mathbf{w}(n)} E\left[\mathbf{w}^T(n)\mathbf{x}(n)\mathbf{x}^T(n)\mathbf{w}(n)\right] \\ &= 2E\left[\mathbf{x}(n)\mathbf{x}^T(n)\mathbf{w}(n)\right] \\ &= 2\mathbf{R}_{xx}\mathbf{w}(n).\end{aligned} \tag{A7}$$

By substituting Eqs. (A6) and (A7) into Eqs. (A3), (A4) and (A5), the final Lagrangian factor is obtained:

$$\lambda_o = \frac{\mathbf{w}_o^T\mathbf{P}_{dx'} - \mathbf{w}_o^T\mathbf{R}_{x'x'}\mathbf{w}_o}{\rho^2} \; or \; 0, \tag{A8}$$

where $\mathbf{w}_o$ is the final optimal solution of the objective function in Eq. (6). If $\lambda_o \neq 0$, Eq. (A8) can be rewritten as

$$\begin{aligned}\lambda_o &= \frac{E\{d(n)\mathbf{w}_o^T\mathbf{X}(n)\mathbf{s}(n) - \mathbf{w}_o^T\mathbf{X}(n)\mathbf{s}(n)\mathbf{s}^T(n)\mathbf{X}^T(n)\mathbf{w}_o\}}{\rho^2} \\ &= \frac{E\{y'_o(n)[d(n) - y'_o(n)]\}}{\rho^2} \\ &= \frac{E[y'_o(n)d(n)] - E[y'_o(n)^2]}{\rho^2}\end{aligned} \quad , \tag{A9}$$

where $y'_o(n) = \mathbf{w}_o^T\boldsymbol{X}(n)\mathbf{s}(n)$. As the final anti-noise $y'_o(n)$ has the same phase with $d(n)$ (residual error $e(n) = d(n) - y'(n)$), and that the amplitude of $d(n)$ is greater than $y'_o(n)$, the expectation $E[y'_o(n)d(n)] - E[y'_o(n)^2]$ will become greater than 0. Hence, the range of Lagrangian factor should be:

$$\lambda_o \geq 0. \tag{A10}$$

Rearranging Eqs. (A3), (A4), (A5), and (A10) yields

$$\begin{cases} \dfrac{\partial L(\mathbf{w}_o, \lambda_o)}{\partial \mathbf{w}_o} = 0; \\ g(\mathbf{w}_o) - \rho^2 \le 0; \\ \lambda_o [g(\mathbf{w}_o) - \rho^2] = 0; \\ \lambda_o \ge 0. \end{cases} \tag{A11}$$

Equation (A11) satisfies the Kuhn-Tucker stationary conditions, which is the necessary condition for Eq. (6) to have an optimal solution [42]. Because the reference signal $x(n)$ inherently incorporates measurement noise, the Hessian matrixes of $J(\mathbf{w})$ and $g(\mathbf{w})$ exist and are positive definite for every $w(n) \in \mathbb{R}$, and hence they are strictly convex on $\boldsymbol{w}(n)$. Therefore, Eq. (6) has only one optimal solution. The optimal solution can be derived from Eq. (A11) as:

$$\mathbf{w}_o = \left(\lambda_o \mathbf{R}_{xx} + \mathbf{R}_{x'x'}\right)^{-1} \mathbf{P}_{dx'}. \tag{A12}$$

### 7.2 Appendix B: Minimum mean square error (MMSE) of the adaptive algorithm with output constraint

Since the error signal $e(n)$ of and active control system is given by

$$e(n) = d(n) - \sum_{l=0}^{L-1} s_l \mathbf{w}^T (n-l) \mathbf{x}(n-l). \tag{B1}$$

The mean square error can be expressed as

$$\begin{aligned} J(\mathbf{w}) &= E\left[ |e(n)|^2 \right] \\ &= E\left[ d(n)^2 \right] - \mathbf{P}_{dx'}^T \mathbf{w}(n) - \mathbf{w}^T(n) \mathbf{P}_{dx'} + \mathbf{w}^T(n) \mathbf{R}_{x'x'} \mathbf{w}(n) \\ &= E\left[ d(n)^2 \right] - 2\mathbf{w}^T(n) \mathbf{P}_{dx'} + \mathbf{w}^T(n) \mathbf{R}_{x'x'} \mathbf{w}(n). \end{aligned} \tag{B2}$$

Also, if $\lambda_o \neq 0$, the third term of Eq. (A11) can be rewritten as

$$
\begin{aligned}
g(\mathbf{w}_o) &= \mathbf{w}_o^T \mathbf{R}_{xx} \mathbf{w}_o \\
&= E\left[ y_o(n)^2 \right]. \\
&= \rho^2
\end{aligned}
\tag{B3}
$$

When the $\mathbf{w}(n) = \mathbf{w}_o$, the second term in Eq. (B2) can be expanded to

$$
\mathbf{w}_o^T \mathbf{P}_{dx'} = \mathbf{w}_o^T \lambda_o \mathbf{R}_{xx} \mathbf{w}_o + \mathbf{w}_o^T \mathbf{R}_{x'x'} \mathbf{w}_o ,
\tag{B4}
$$

and the third term in Eq. (B2) can be derived as

$$
\begin{aligned}
\mathbf{w}_o^T \mathbf{R}_{x'x'} \mathbf{w}_o &= \left\| S(e^{j\omega}) \right\|_2^2 E\left[ y_o(n)^2 \right] \\
&= \frac{1}{2\pi} \int_{-\pi}^{\pi} \left| S(e^{j\omega}) \right|^2 d\omega \times \rho^2 \\
&= \sum_{i=0}^{L-1} s_i^{\,2} \rho^2
\end{aligned}
\tag{B5}
$$

Substituting Eqs. (B3), (B4), and (B5) into Eq. (B2), the minimal mean square error should be

$$
\begin{aligned}
J_{\min}(\mathbf{w}_o) &= E\left[ d(n)^2 \right] - 2\mathbf{w}_o^T \mathbf{P}_{dx'} + \mathbf{w}_o^T \mathbf{R}_{x'x'} \mathbf{w}_o \\
&= E\left[ d(n)^2 \right] - 2\lambda_o \mathbf{w}_o^T \mathbf{R}_{xx} \mathbf{w}_o - \mathbf{w}_o^T \mathbf{R}_{x'x'} \mathbf{w}_o \\
&= E\left[ d(n)^2 \right] - \left( \sum_{l=0}^{L-1} s_l^2 + 2\lambda_o \right) \rho^2 .
\end{aligned}
\tag{B6}
$$

From Eq. (A10), we can figure out that $\lambda_o$ has a non-negative value. If $\lambda_o$ equals to 0, Eq. (B6) will become

$$
J_{\min} \approx E\left[ d(n)^2 \right] - \sum_{l=0}^{L-1} s_l^2 \rho^2 \ .
\tag{B7}
$$

## Acknowledgement

This material is based on research/work supported by Singapore Ministry of National Development and National Research Foundation under L2 NIC Award ($\mathrm{NO.\,L2NICCFP1} - 2013 - 7$).

**Reference**

[1] B. Widrow, C.S. Williams, J.R. Glover, J.M. McCool, R.H. Hearn, J.R. Zeidler, J. Kaunitz, E. Dong, R.C. Goodlin, C.S. Williams, R.H. Hearn, J.R. Zeidler, J.E. Dong, R.C. Goodlin, Adaptive Noise Cancelling: Principles and Applications, Proc. IEEE. 63 (1975) 1692–1716. doi:10.1109/PROC.1975.10036.

[2] C.N. Hansen, Understanding active noise cancellation, CRC Press, 2002.

[3] Y. Kajikawa, W.-S. Gan, S.M. Kuo, Recent advances on active noise control: open issues and innovative applications, APSIPA Trans. Signal Inf. Process. 1 (2012). doi:10.1017/ATSIP.2012.4.

[4] S.M. Kuo, D.R. Morgan, Active noise control: a tutorial review, Proc. IEEE. 87 (1999) 943–973. doi:10.1109/5.763310.

[5] S.J. Elliott, P.A. Nelson, Active Noise Control, IEEE Signal Process. Mag. 10 (1993) 12–35. doi:10.1109/79.248551.

[6] D. Shi, C. Shi, W.S. Gan, A systolic FxLMS structure for implementation of feedforward active noise control on FPGA, in: 2016 Asia-Pacific Signal Inf. Process. Assoc. Annu. Summit Conf. APSIPA 2016, 2017. doi:10.1109/APSIPA.2016.7820755.

[7] C. Liu, Z. Zhang, X. Tang, Sign normalised spline adaptive filtering algorithms against impulsive noise, Signal Processing. 148 (2018) 234–240.

[8] D. Shi, C. Shi, W.S. Gan, Effect of the Audio Amplifier's Distortion on Feedforward

Active Noise Control, in: 2017 Asia-Pacific Signal Inf. Process. Assoc. Annu. Summit Conf., 2017.

[9] M.H. Costa, J.C.M. Bermudez, N.J. Bershad, Stochastic analysis of the LMS algorithm with a saturation nonlinearity following the adaptive filter output, IEEE Trans. Signal Process. 49 (2001) 1370–1387. doi:10.1109/78.928691.

[10] F. Taringoo, J. Poshtan, M.H. Kahaei, Analysis of effort constraint algorithm in active noise control systems, EURASIP J. Adv. Signal Process. 2006 (2006) 54649.

[11] S.J. Elliott, C.C. Boucher, P.A. Nelson, The behavior of a multiple channel active control system, IEEE Trans. Signal Process. 40 (1992) 1041–1052. doi:10.1109/78.134467.

[12] N. V. George, G. Panda, Advances in active noise control: A survey, with emphasis on recent nonlinear techniques, Signal Processing. 93 (2013) 363–377. doi:10.1016/j.sigpro.2012.08.013.

[13] L.-Z. Tan, J. Jiang, Filtered-X second-order Volterra adaptive algorithms, Electron. Lett. 33 (1997) 671–672. doi:10.1049/el:19970477.

[14] Y. Kajikawa, Adaptive Volterra filter: its present and future, Electron. Commun. Japan, Part III Fundam. Electron. Sci. (English Transl. Denshi Tsushin Gakkai Ronbunshi). 83 (2000) 51–61. doi:10.1002/1520-6440(200012)83:12<51::AID-ECJC6>3.0.CO;2-K.

[15] J.C. Patra, R.N. Pal, B.N. Chatterji, G. Panda, Identification of nonlinear dynamic systems using functional link artificial neural networks., IEEE Trans. Syst. Man. Cybern. B. Cybern. 29 (1999) 254–262. doi:10.1109/3477.752797.

[16] Q. Zhang, Y. Jia, Active noise hybrid feedforward/feedback control using neural

network compensation, J. Vib. Acoust. 124 (2002) 100–104.

[17] P. Li, X. Bai, Y. Ma, Two kinds of active impulsive noise control algorithms based on sigmoid transformation, in: Seventh Int. Conf. Electron. Inf. Eng., 2017: p. 103220R--103220R.

[18] C.-Y. Chang, K.-K. Shyu, Active noise cancellation with a fuzzy adaptive filtered-X algorithm, IEE Proceedings-Circuits, Devices Syst. 150 (2003) 416–422.

[19] J.M. Sousa, C.A. Silva, J.M.G. Sá da Costa, Fuzzy active noise modeling and control, Int. J. Approx. Reason. 33 (2003) 51–70. doi:10.1016/S0888-613X(02)00147-0.

[20] X. Qiu, C.H. Hansen, A study of time-domain FXLMS algorithms with control output constraint, J. Acoust. Soc. Am. 109 (2001) 2815–2823.

[21] W.J. Kozacky, T. Ogunfunmi, Convergence Analysis of an Adaptive Algorithm With Output Power Constraints, IEEE Trans. Circuits Syst. II Express Briefs. 61 (2014) 364–367. doi:10.1109/TCSII.2014.2312637.

[22] Z. Zhang, F. Hu, J. Wang, On saturation suppression in adaptive vibration control, J. Sound Vib. 329 (2010) 1209–1214. doi:10.1016/j.jsv.2009.11.027.

[23] W.J. Kozacky, T. Ogunfunmi, An adaptive IIR filter with constraints on the output power level, in: Signals, Syst. Comput. (ASILOMAR), 2010 Conf. Rec. Forty Fourth Asilomar Conf., 2010: pp. 984–987.

[24] O.J. Tobias, R. Seara, Leaky-FXLMS algorithm: Stochastic analysis for Gaussian data and secondary path modeling error, IEEE Trans. Speech Audio Process. 13 (2005) 1217–1230. doi:10.1109/TSA.2005.852018.

[25] O.J. Tobias, R. Seara, On the LMS algorithm with constant and variable leakage factor

in a nonlinear environment, IEEE Trans. Signal Process. 54 (2006) 3448–3458. doi:10.1109/TSP.2006.879274.

[26] S.J. Elliott, K.H. Back, Effort constraints in adaptive feedforward control, IEEE Signal Process. Lett. 3 (1996) 7–9. doi:10.1109/97.475821.

[27] B. Rafaely, S.J. Elliot, A computationally efficient frequency-domain LMS algorithm with constraints on the adaptive filter, IEEE Trans. Signal Process. 48 (2000) 1649–1655. doi:10.1109/78.845922.

[28] W.J. Kozacky, T. Ogunfunmi, An active noise control algorithm with gain and power constraints on the adaptive filter, EURASIP J. Adv. Signal Process. 2013 (2013) 17.

[29] X. Qiu, C.H. Hansen, Applying effort constraints on adaptive feedforward control using the active set method, J. Sound Vib. 260 (2003) 757–762.

[30] H. Lan, M. Zhang, W. Ser, A weight-constrained FxLMS algorithm for feedforward active noise control systems, IEEE Signal Process. Lett. 9 (2002) 1–4. doi:10.1109/97.988714.

[31] W.H. Swann, A survey of non-linear optimization techniques, FEBS Lett. 2 (1969) S39--S55. doi:10.1016/0014-5793(69)80075-X.

[32] A. Rothwell, Optimization Methods in Structural Design, (2017).

[33] S.M. Roberts, H.I. Lyvers, The gradient method in process control, Ind. Eng. Chem. 53 (1961) 877–882.

[34] D.R. Morgan, History, applications, and subsequent development of the FXLMS algorithm, IEEE Signal Process. Mag. 30 (2013) 172–176. doi:10.1109/MSP.2013.2242394.

[35] C.Y. Chang, S.M. Kuo, C.W. Huang, Secondary path modeling for narrowband active noise control systems, Appl. Acoust. 131 (2018) 154–164. doi:10.1016/j.apacoust.2017.10.026.

[36] E. Bjarnason, Analysis of the Filtered-X LMS Algorithm, IEEE Trans. Speech Audio Process. 3 (1995) 504–514. doi:10.1109/89.482218.

[37] L. Wu, X. Qiu, Y. Guo, A generalized leaky FxLMS algorithm for tuning the waterbed effect of feedback active noise control systems, Mech. Syst. Signal Process. 106 (2018) 13–23.

[38] National-Instrument, Least Mean Squares (LMS) Algorithms (Adaptive Filter Toolkit), (2008). http://zone.ni.com/reference/en-XX/help/372357A-01/lvaftconcepts/aft_lms_algorithms/.

[39] B. Widrow, S. Stearns, Adaptive Signal Processing, in: Adapt. Signal Process., 1985: p. 11. doi:10.1002/9780470575758.

[40] W.J. Kozacky, T. Ogunfunmi, A cascaded IIR-FIR adaptive ANC system with output power constraints, Signal Processing. 94 (2014) 456–464. doi:10.1016/j.sigpro.2013.06.036.

[41] S.M. Kuo, H.-T.-T. Wu, F.-K.-K. Chen, M.R. Gunnala, Saturation effects in active noise control systems, IEEE Trans. Circuits Syst. I Regul. Pap. 51 (2004) 1163–1171. doi:10.1109/TCSI.2004.829241.

[42] M.A. Hanson, On sufficiency of the Kuhn-Tucker conditions, J. Math. Anal. Appl. 80 (1981) 545–550.

[43] S.S. Haykin, Adaptive filter theory, Pearson Education India, 2008.

[44] S.M. Kuo, D. Morgan, Active noise control systems: algorithms and DSP implementations, John Wiley & Sons, Inc., 1995.

[45] T. Hsia, Convergence analysis of LMS and NLMS adaptive algorithms, IEEE Int. Conf. Acoust., Speech, Signal Process. 8 (1983) 667–670. doi:10.1109/ICASSP.1983.1172047.

[46] S.C. Douglas, A Family of Normalized Lms Algorithms, IEEE Signal Process. Lett. 1 (1994) 49–51. doi:10.1109/97.295321.

[47] C.Y. Chang, Efficient active noise controller using a fixed-point DSP, Signal Processing. 89 (2009) 843–850. doi:10.1016/j.sigpro.2008.10.025.

[48] K. Shyu, C. Ho, C. Chang, A Study on Using Microcontroller to Design Active Noise Control Systems, (2014) 443–446.

[49] C.Y. Chang, S.T. Li, Active noise control in headsets by using a low-cost microcontroller, IEEE Trans. Ind. Electron. 58 (2011) 1936–1942. doi:10.1109/TIE.2010.2058071.

[50] H.S. Vu, K.H. Chen, A High-Performance Feedback FxLMS Active Noise Cancellation VLSI Circuit Design for In-Ear Headphones, Circuits, Syst. Signal Process. 36 (2017) 2767–2785. doi:10.1007/s00034-016-0436-y.

[51] D.M. Harris, S.L. Harris, Digital Design and Computer Architecture, 2007. doi:10.1016/B978-0-12-370497-9.X5000-8.

[52] R.K. Dueck, R.K. Dueck, Digital design with CPLD applications and VHDL, Books.Google.Com. (2005) 841.

[53] J. Dattorro, J. Dattorro, Convex Optimization and Euclidean Distance Geometry, (2009).